Available online at www.sciencedirect.com
SCIENCE DIRECT®
Journal of Magnetism and Magnetic Materials 300 (2006) 159–163
Journal of magnetism and magnetic materials
www.elsevier.com/locate/jmmm

Micromagnetic simulations of the magnetization dynamics in nanostructures with special applications to spin injection

D.V. Berkov*

INNOVENT Technology Development, Prüssingstr. 27B, Jena D-07745, Germany

Available online 17 November 2005

Abstract

We present several micromagnetic simulation examples of magnetization dynamics driven by the spin injection. First, we address the validity of the macrospin approximation often used to interpret experimental data. Next, we discuss the interpretation of experimental results obtained on columnar multilayer structures and show that a sophisticated micromagnetic model which takes into account a polycrystalline structure of a nanoelement can explain qualitatively the most important features of the magnetization oscillation spectra observed experimentally. A quantitative agreement with experimental results, however, could not be achieved in the region of reasonable parameter values. The third part of our contribution deals with simulations of the point-contact experiments. Here, we find an important qualitative disagreement between the experiment and simulations. The latter predict the existence of *two* current regions of a steady-state precession of the point-contact area (before and after spin-polarized current-driven magnetization switching), whereas experimentally only one such region is observed. In conclusion, we discuss some explanations of the above-mentioned discrepancies.

PACS: 85.75.−d; 75.75.+a; 75.40.Gb; 75.40.Mg

Keywords: Spin injection; Micromagnetic simulations; Steady-state precession; Magnetization switching

1. Introduction

Theoretical predictions of the possibility to induce magnetic excitations in a thin film and even switch a nanoelement magnetization using a DC spin-polarized current (SPC) [1,2] have led to a formation of a new research area in a solid-state magnetism devoted to the interaction of an electric current with spin-polarized carriers with the magnetization of a ferromagnetic body. After first successful experiments where such an interaction was observed [3,4] several very promising applications of this phenomenon have been suggested [5], which employ as well DC-current-induced magnetic excitations (microwave generators), as SPC-induced switching (MRAM-cells, GMR-heads).

Development of such devices requires a thorough understanding of the underlying physics, even if one leaves apart that spin-injection phenomena are highly interesting from the fundamental point of view. In the recent years, an immense theoretical effort was devoted to the elaboration of the corresponding theories both on the quantum mechanical and phenomenological basis (see, e.g., Ref. [6]). At the same time quantitative experiments could be performed on relatively good characterized magnetic systems, so that a meaningful comparison of theoretical predictions with experimental data became possible.

Such a comparison, however, cannot be made based on the analytical *microscopic* theories only, because such theories take no account of the complicated magnetization configurations in nanoelements. All experimental data are obtained on structures larger than the single-domain threshold, so that effects of a non-collinear magnetization state must be included to enable a quantitative (and often even a qualitative) comparison between theory and measurements.

Micromagnetic simulations provide in principle an ideal tool to bridge the gap between the microscopic theories of a spin-transfer and high-quality measurements on magnetic nanolayers, being able to include additional torque terms

*Tel.: +49 3641 282537; fax: +49 3641 282530.
E-mail address: db@innovent-jena.de.

0304-8853/$ - see front matter © 2005 Elsevier B.V. All rights reserved.
doi:10.1016/j.jmmm.2005.10.055

(derived from theoretical considerations) into the mesoscopic equations of motion [7]. Solution of these equations for systems of experimentally observable sizes [8–10] allows a meaningful quantitative comparison mentioned above. Below we discuss several corresponding examples.

2. Validity of a single-domain approximation

Before we proceed with the analysis of the full-scale micromagnetic simulations, it is useful to recapitulate the important issue concerning the applicability of the macrospin (single-domain) approximation to the simulations of spin-transfer phenomena.

The derivation of a single-domain critical size usually relies on the comparison between the closed-flux magnetization configurations having the exchange energy E_{exch} only and the collinear state with the stray-field energy E_{dem} (see Chapter 3.3 in Ref. [11] for details). The exchange energy density increases with decreasing particle size, leading to the result that below a critical size l_{cr} which scales with the exchange length $l_{\text{exch}} = (A/2\pi M_{\text{S}}^2)^{1/2}$ only a collinear magnetization state is thermodynamically stable. Exact value of l_{cr} depends on the particle shape and on the non-collinear state used to compute E_{exch}, and in most cases $l_{\text{cr}} \simeq (4-8)l_{\text{exch}}$ [11]. The exchange length $l_{\text{exch}} \approx 5\,\text{nm}$ or less for most ferromagnets, so that an *upper* border for the single-domain threshold is $l_{\text{cr}} \approx 40\,\text{nm}$. This would mean that for nearly all experiments (leaving aside data obtained on point contacts, see discussion below) the lateral element size is far above l_{cr}, making a macrospin approximation invalid.

Several complicated circumstances have to be taken into account, however. First, the l_{cr}-estimate obtained based on the *energy* comparison of different configurations cannot be used to predict whether the transition to a multidomain state will *really* occur during the remagnetization, because this transition often requires surmounting of a relatively high energy barrier. Simulations have shown that for certain particle shapes almost collinear magnetization states persist during the whole remagnetization process in a *homogeneous* external field for nanoelements with lateral sizes as large as several hundred nanometers.

On the other hand, most calculations leading to the estimation $l_{\text{cr}} \simeq (4-8)l_{\text{exch}}$given above were performed for particles with all three dimensions having the same order of magnitude (cubes, spheres, etc.). For a thin-film element with the thickness much smaller than its lateral sizes the exchange and stray-field energies might have a different dependence on the element size than for a 'really 3D' particle, which might substantially alter the critical size l_{cr}.

The next consideration is specific for SPC-induced remagnetization processes. The additional torque emerging in the LLG equation due to the SPC injection has the form $\mathbf{N}_{\text{SPC}} \sim [\mathbf{M} \times [\mathbf{S} \times \mathbf{M}]]$ [1,6], so that the corresponding effective field contribution $\mathbf{H}_{\text{SPC}} \sim [\mathbf{S} \times \mathbf{M}]$ (strictly speaking, this torque cannot be reduced to an effective field, but for our qualitative analysis we can use this analogy). For example, a square nanoelement in a '*flower*' remanent state and the spin polarization $\mathbf{S}$ along (or antiparallel to) its mean magnetization direction additional spin torque fields $\mathbf{H}_{\text{SPC}} \sim [\mathbf{S} \times \mathbf{M}]$ have *opposite* directions near the adjacent corners of this nanoelement. Up to some extent this is equivalent to the remagnetization of an element in a *strongly inhomogeneous* external field, which favors the formation of a multidomain structure (see corresponding discussion in Ref. [12]).

The line of arguments presented above mean that each specific experimental situation requires a separate micromagnetic analysis to find out whether the macrospin approximation is valid for its description. An example of such an analysis is given in our paper [13], where we have studied an SPC-induced precession in a square element with the thickness $h = 2.5\,\text{nm}$ and typical magnetic parameters ($M_{\text{S}} \approx 1000\,\text{G}$, $A = 2 \times 10^{-6}\,\text{erg/cm}$). We have shown than the magnetization configuration during such a precession significantly deviates from the single-domain one already for lateral sizes as small as $b = 30-40\,\text{nm}$, which is significantly smaller than in all experiments reported up to now for the columnar multilayer systems.

The last important remark concerning the macrospin approximation concerns the proper interpretation of point-contact experiments. In such experiments, the size of the area flooded by a current through a 'free' magnetic layer can be as small as 25 nm [14], making it very tempting to declare that the macrospin approximation is applicable to analyze these experiments even quantitatively. Unfortunately, at present there exist no adequate method to incorporate the strong exchange interaction of the area under the contact with the rest of the layer. Hence, the macrospin model is, strictly speaking, invalid in this experimental situation for any size of the point contact.

3. Simulations of the steady-state precession for a thin elliptical monolayer element

The first typical experimental setup where SPC-induced magnetization excitations were observed is a columnar geometry where an electric current flows through a columnar multilayer structure consisting of different magnetic layers separated by non-magnetic spacers [15–17].

Several very interesting results on this setup were reported by the Cornell group [16,17]. In particular, Kiselev et al. [16] have found the following qualitative features of the steady-state microwave magnetization excitations in Co/Cu/Co pillars: (i) several equidistant spectral bands exist for a large range of DC currents, (ii) there exist at least two oscillation regimes called by the authors of [16] 'small-angle' and 'quasichaotic' oscillations, (iii) the 'small-angle' oscillation power is at least one order of magnitude smaller than in the 'quasichaotic' regime and (iv) the frequency of 'small-angle' oscillations is more than two times larger than of the 'quasichaotic' ones.

We have simulated these experiments modeling the system from Ref. [16] by a single-layer elliptical element

with lateral sizes $a \times b = 130 \times 70\,\mathrm{nm}^2$ and thickness $h = 3\,\mathrm{nm}$. Neglecting the magnetodipolar interaction with the lower extended thick Co layer should be a good approximation: the lateral sizes of the thick layer were much larger than those of the 'free' layer thus strongly reducing the stray-field coupling at least in the equilibrium.

Simulations were performed using our commercially available package MicroMagus [18] with an add-on spin-injection module which adds the Slonczewski torque $\mathbf{N}_{\mathrm{SPC}} = a_J[\mathbf{M} \times [\mathbf{S} \times \mathbf{M}]]$ to the LLG equation of motion (the factor a_J is proportional to the current strength). The element was discretized in plane into cells with lateral sizes $2.5 \times 2.5\,\mathrm{nm}^2$. The only important methodical point by simulations of this system is the mandatory usage of an equation-of-motion integrator with a *build-in step-size control*, because due to the complicated character of the magnetization oscillations (especially quasichaotic ones) very different time steps are required for various magnetization states to maintain the prescribed integration accuracy.

Simulation results obtained for the 'minimal' micromagnetic model (neglecting both a polycrystalline structure of the Co layer and thermal fluctuations) are shown in Fig. 1. Here, the saturation magnetization of the 'free' Co layer $4\pi M_S = 10\,\mathrm{kG}$ [16] and the exchange constant $A = 3 \times 10^{-6}$ [19,20] were used. Oscillation power spectra of the magnetization components were extracted from the time dependencies of these components using the Lomb algorithm, which allows one to handle data spaced unevenly in time.

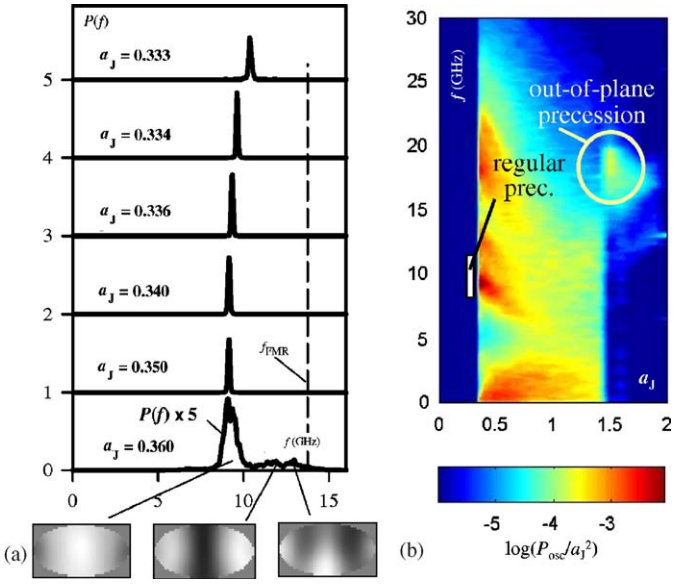

Fig. 1. (a) Oscillation power spectra (OPS) of the *in-plane* magnetization component perpendicular to the long ellipse axis for *low* current values a_J. Spatial mode structures for a_J just above the transition to a quasichaotic regime are shown. (b) Magnetoresistance OPS in the whole a_J range. Area corresponding to regular precession shown in (a) is marked by a small white rectangle. Several spectral bands and a significant region of the out-of-plane precession can be clearly seen.

The 'minimal' model can explain some qualitative features of the results from Ref. [16]. In particular, we have also found regular (for small currents, Fig. 1a) and quasichaotic (for larger a_J, Fig. 1b) oscillation regimes. Several spectral bands observed for a quasichaotic regime (Fig. 1b) are due to the superposition of the oscillation signals from the in-plane magnetization components which are perpendicular (m_y) and along (m_x) the long ellipse axis, because for the precession in this geometry the m_x-precession frequency is two times larger than for the m_y-precession.

However, important disagreement with the experimental results should be pointed out. First, the region of regular oscillations is extremely narrow, in contrast to a relatively broad current range for 'small-angle' oscillations in Ref. [16]. Second, the regular oscillation power is at least comparable with that in the quasichaotic regime. Third, the frequency of regular oscillations is nearly the same as at the beginning of the quasichaotic regime. And finally, simulations predict the existence of a relatively broad region of 'out-of-plane' oscillations not observed experimentally.

To find out, whether the agreement can be improved using a more sophisticated model within a 'standard' micromagnetic formalism, we have built in a polycrystalline structure with the average lateral crystallite size $\langle D \rangle = 10\,\mathrm{nm}$ and various anisotropy kinds (thin Co films may possess FCC or HCP structures dependent on the film thickness and the preparation method [21,22]). Detailed simulation results for such a polycrystalline element and comparison with other numerical simulation studies [9,10] are reported elsewhere [23]. Summarizing, we have found that the cubic FCC anisotropy (with randomly oriented grain anisotropy axes) slightly expands the regular precession region and strongly decreases the out-of-plane oscillation power, also narrowing the current region of its existence. Precession frequencies and the relation between the oscillation powers in regular and quasichaotic regimes were affected only slightly.

In contrast to the former case, the introduction of the uniaxial HCP anisotropy (which constant is much higher than for the FCC case [24]) resulted in the *qualitative* changes in the oscillation spectra, although due to the very small crystallite size the random anisotropy effect is largely 'averaged out' [25]. The major new feature of 'samples' with the HCP crystallites is a strong variation of the power spectra for samples with different realizations of the random grain structure (Fig. 2). This variation is due to the strong local influence of the HCP anisotropy which also leads to the spatial localization of the magnetization oscillations in different sample parts for regular and quasichaotic oscillations. Depending on the relation between these localization areas and the corresponding local anisotropy directions, we could observe very different ratios between the frequencies and oscillation power in regular and quasichaotic regimes, which for some samples were quite close to those observed experimentally [16]. Taking into account that the sputtered thin Co films exhibit

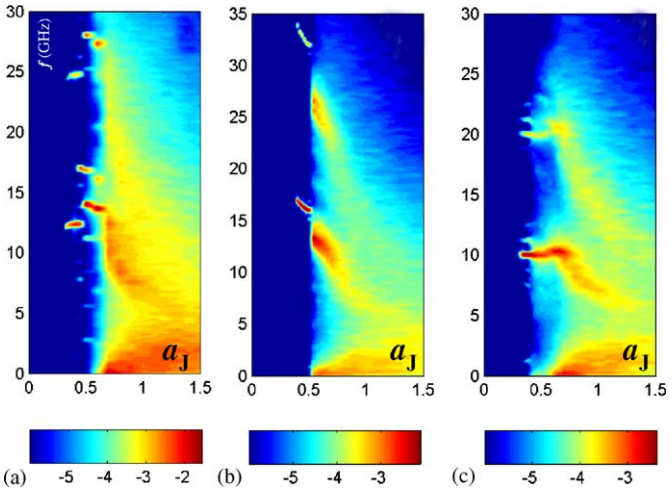

Fig. 2. Magnetoresistance OPS in the whole a_J range for samples with identical microscopic parameters but *different* realizations of the random HCP crystallite structure.

a mixed FCC/HCP crystallographic structure with predominantly FCC grains [22], the random polycrystalline anisotropy could provide a natural explanation for the experimentally observed features mentioned at the beginning of this section. However, an important quantitative disagreement with the experimental data still exits: the frequency of quasichaotic oscillations obtained numerically ($\approx$9–10 GHz) is significantly higher than measured experimentally ($\approx$6.5 GHz).

4. Analysis of the magnetization oscillations in a point-contact geometry

An alternative experimental setup for the excitation of magnetization oscillation with a DC-SPC is the point-contact geometry [27]. Here, a current is injected into a metallic multilayer (also composed of two magnetic layers separated by a non-magnetic spacer) via a point contact. The contact diameter should be very small (maximum several tenth of nanometers) to ensure that the spin-transfer dominates over the Oersted field effect. The lateral size of magnetic layers in this setup is about several micrometers, so that compared to the point-contact diameter they can be safely treated as infinitely extended.

Micromagnetic simulations of spin wave excitations in this geometry encounter serious methodical problems. First, the lateral size of magnetic layers is too large to simulate the whole system, so that periodic boundary conditions (PBC) should be used. Due to PBC the spin waves emitted by the system replica can enter the simulation area and cause substantial artificial interference with the 'primary' waves, especially taking into account that they have the same frequencies. Second, numerical approximation of the area which is flooded by the current becomes non-trivial: a straightforward approach where this area is approximated as a circle with a sharp border leads to artificial magnetization oscillations with very short wavelengths due to corresponding special oscillations of the Fourier transform of abruptly changing spatial structures. Detailed solutions of these problems will be presented elsewhere.

We have performed simulations of a multilayer system similar to that studied in Ref. [27]: a Py(5 nm)/Cu(5 nm)/$Co_{90}Fe_{10}$(10 nm) sandwich with the saturation magnetization for Py M_S(Py) = 640 G [27] and M_S(CoFe) = 1500 G [26]. Exchange constants were set to $A(\mathrm{Py}) = 1 \times 10^{-6}$ erg/cm and $A(\mathrm{CoFe}) = 2 \times 10^{-6}$ erg/cm. The lateral size of the simulated area was 0.8×1.2 mkm and each magnetic layer was discretized in plane into $2.5 \times 2.5\,\mathrm{nm}^2$ cells.

Simulation results show an important *qualitative* disagreement with the experimental data from Ref. [27]. Namely, we have found *two* current regions where steady-state magnetization oscillations take place.

The first region (Fig. 3) corresponds to the DC-current strength for which the oscillating magnetization of the free (Py) layer area under the point contact is directed approximately *along* the magnetization of the fixed (CoFe) layer. The oscillation frequency in this regime slightly decreases with the increased current (in agreement with Ref. [27]), but its absolute value $f_{\mathrm{sim}} \approx 10.5$ GHz is significantly above the experimental value $f_{\mathrm{exp}} \approx 7.5$ GHz.

When the current was increased above the critical value corresponding to the *switching* of the magnetization under the point-contact area, we have found the *second* region of stable steady-state magnetization excitations where the magnetization was oscillating around the direction of the

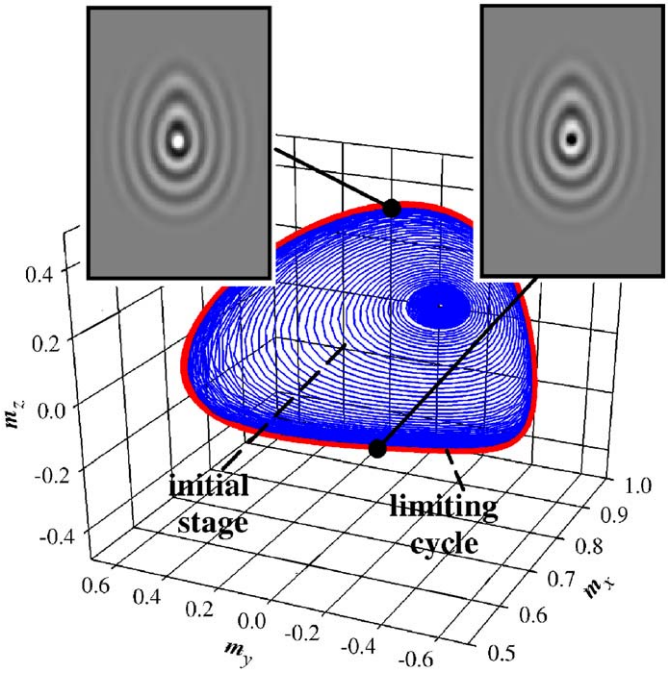

Fig. 3. Magnetization oscillations in the point-contact geometry for the current *below* the switching threshold. 3D magnetization trajectory and gray-scale maps for the magnetization projection perpendicular to the layer plane are shown.

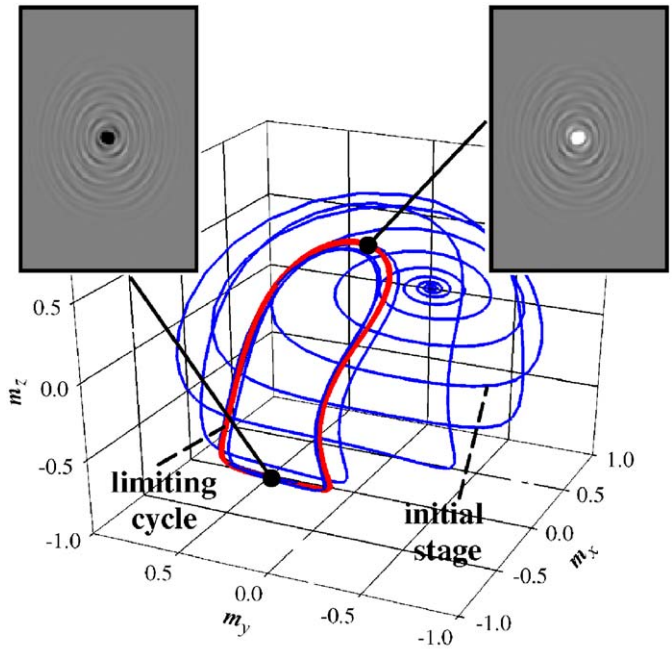

Fig. 4. Same as in Fig. 3 for the current *above* the switching threshold. The simplest magnetization configuration is shown.

spin polarization, i.e., around the direction *opposite* to the magnetization of the 'free' layer outside the point-contact area (Fig. 4). The frequency of these oscillations was roughly two times smaller than for the first region (what is a natural consequence of the fact that for a switched region the external field and the exchange interaction field have opposite directions) and its dependence on the current strength was very weak. Spatial mapping of magnetization components revealed that in this regime a sharp change of the magnetization direction on the border of the oscillating area takes place in contrast to oscillations before switching.

The reasons of important disagreements found both for a columnar and point-contact geometries may be (i) the increase of the magnetization damping in the presence of spin-transfer processes and (ii) the damping dependence on the instantaneous magnetization configuration [28–30]. These effects can be especially pronounced in the point-contact experiments, where the current density required to induce magnetic excitations is much higher than for the columnar geometry. And indeed, the disagreement between simulations (where the constant damping with the small values usually assumed for bulk magnetic materials is used) and experimental data are much more significant for the point-contact experimental setup.

References

[1] J.C. Slonczewski, J. Magn. Magn. Mater. 159 (1996) L1.
[2] L. Berger, Phys. Rev. B 54 (1996) 9353.
[3] J.Z. Sun, J. Magn. Magn. Mater. 202 (1999) 157.
[4] M. Tsoi, A.G.M. Jansen, J. Bass, W.-C. Chiang, M. Seck, V. Tsoi, P. Wyder, Phys. Rev. Lett. 80 (1998) 4281.
[5] G. Reiss, H. Brueckl, A. Huetten, J. Schmalhorst, M. Justuts, A. Thomas, S. Heitman, Phys. Status Solidi B 236 (2003) 289.
[6] D.M. Apalkov, P.B. Visscher, J. Magn. Magn. Mater. 286 (2005) 370.
[7] J.Z. Sun, Phys. Rev. B62 (2000) 570.
[8] Z. Li, S. Zhang, Phys. Rev. B68 (2003) 024404.
[9] J.-G. Zhu, X. Zhu, IEEE Tarns. Magn. 40 (2004) 182.
[10] K.J. Lee, A. Deac, O. Redon, J.P. Nozieres, B. Dieny, Nat. Mater. 3 (2004) 877.
[11] A. Hubert, R. Schäfer, Magnetic Domains, Springer, Berlin, 1998.
[12] J. Miltat, G. Albuquerque, A. Thiaville, C. Vouille, J. Appl. Phys. 89 (2001) 6982.
[13] D.V. Berkov, N.L. Gorn, Phys. Rev. B71 (2005) 052403.
[14] W.H. Rippard, M.R. Pufall, S. Kaka, S.E. Russek, T.J. Silva, Phys. Rev. Lett. 92 (2004) 027201.
[15] J.A. Katine, F.J. Albert, R.A. Buhrman, E.B. Myers, D.C. Ralph, Phys. Rev. Lett. 84 (2000) 3149.
[16] S.I. Kiselev, J.C. Sankey, I.N. Krivorotov, N.C. Emley, R.J. Schoelkopf, R.A. Buhrman, D.C. Ralph, Nature 425 (2003) 380.
[17] S.I. Kiselev, J.C. Sankey, I.N. Krivorotov, N.C. Emley, M. Rinkoski, C. Perez, R.A. Buhrman, D.C. Ralph, Phys. Rev. Lett. 93 (2004) 036601.
[18] D.V. Berkov, N.L. Gorn, MicroMagus—package for micromagnetic simulations, 〈http:\\www.micromagus.de〉.
[19] G. Shirane, V.J. Minkiewicz, R. Nathans, J. Appl. Phys. 39 (1968) 383.
[20] A. Michels, J. Weissmüller, A. Wiedenmann, J.S. Pedersen, J.G. Barker, Philos. Mag. Lett. 80 (2000) 785.
[21] K. Heinz, S. Müller, L. Hammer, J. Phys.: Cond. Matt. 11 (1999) 9437.
[22] J. Langer, R. Mattheis, B. Ocker, W. Mass, S. Senz, D. Hesse, J. Kräusslich, J. Appl. Phys. 90 (2001) 5126.
[23] D.V. Berkov, N.L. Gorn, Phys. Rev. B 72 (2005) 094401.
[24] D. Weller, G.R. Harp, R.F.C. Farrow, A. Cebollada, J. Sticht, Phys. Rev. Lett. 72 (1994) 2097.
[25] G. Herzer, Nanocrystalline soft magnetic alloys, in: K. Buschov (Ed.), Handbook of Magnetic Materials, vol. 10, Elsevier Science, Amsterdam, 1997.
[26] S.H. Liao, IEEE Trans. Magn. MAG-23 (1987) 2981.
[27] W.H. Rippard, M.R. Pufall, S. Kaka, T.J. Silva, S.E. Russek, Phys. Rev. B 70 (2004) 100406(R).
[28] Y. Tserkovnyak, A. Brataas, G. Bauer, Phys. Rev. Lett. 88 (2002) 117601.
[29] B. Heinrich, G. Woltersdorf, R. Urban, E. Simanek, J. Appl. Phys. 93 (2003) 7545.
[30] Y. Tserkovnyak, A. Brataas, G. Bauer, J. Appl. Phys. 93 (2003) 7534.